Identification of the Active Constituents and Significant Pathways of Bushen Huoxue Decoction for the Treatment of Recurrent Spontaneous Abortion Based on Network Pharmacology

Meihe LI
Capital Medical University Affiliated Beijing Hospital of Traditional Chinese Medicine: Beijing Hospital of Traditional Chinese Medicine
Jinping WU
521 hospital of norinco group
Minchao KANG
Xi'an jiaotong University health science center
Ying XU
xi'an jiaotong university second affiliated hospital
Xin XU
capital medical university of Beijing traditional Chinese Medicine hospital
Huimin DANG (wbb.23@163.com)
Xi'an Jiaotong University Second Affiliated Hospital

Research

Keywords: Bushen Huoxue Decoction, recurrent spontaneous abortion, network pharmacology, Pharmacological mechanism, RStudio

Posted Date: December 31st, 2020

DOI: https://doi.org/10.21203/rs.3.rs-137378/v1

Abstract

Background: To explore Bushen Huoxue Decoction (BHD) mechanism in recurrent spontaneous abortion (RSA).

Methods: We predicted and screened the action targets of four Traditional Chinese Medicine representatives by Traditional Chinese Medicine Systems Pharmacology Database and Analysis Platform, and searched the disease targets of RSA through Drugbank, DisGeNET, and TTD databases. According to the obtained drug targets and disease targets, the "drug target-disease target" interaction network was further analyzed and constructed. The core target of BHD for treating RSA was were imported to establish in STRING. GO and KEGG pathway analysis were conducted with the RStudio (ggplot2). Finally, HTR-8/SVneo cells were selected to establish a cell model of oxidative stress, and the network pharmacologic results of BHD-RSA were verified by cell biology, Western blot and qRT-PCR.

Results: A total of 73 active compounds were obtained from 1084 ingredients present in the BHD, and 125 genes were closely related to RSA. According to the "drug target-disease target" interaction network analysis, 26 core targets of BHD for treating RSA were finally selected, and 203 biological processes, 10 molecular functions, and 10 cell components were enriched by GO function enrichment. KEGG pathway enrichment related pathways, a total of 19, are mainly associated with a Neuroactive ligand-receptor interaction pathway. Experimental results show that compared with the oxidative stress cell model of RSA, BHD increases the expression of PTGFR, AGTR1 and OXTR mRNA by upregulating the expression of PTGFR, AGTR1 and OXTR protein, which may interfere with the occurrence and development of RSA through Neuroactive ligand-receptor interaction pathway.

Conclusion: Combined with the pathological mechanism of RSA and the absence of specific signaling pathways, we hypothesized that the BHD might play a role in tonifying the kidney, strengthening the bone, promoting blood circulation, and removing blood stasis，it also can virtually relieve the symptoms of RSA, and our network pharmacological analysis lays the foundation for future clinical research.

These results may help define the possible roles the BHD plays in RSA through Neuroactive ligand-receptor interaction pathway.

1 Introduction

Recurrent spontaneous abortion (RSA), occurring in 1% of fertile couples(1, 2), is a pregnancy complication with a heterogeneous nomenclature (recurrent pregnancy loss, recurrent miscarriage, habitual abortion) and definition (3). RSA is defined as three or more consecutive abortions with the same partner (1, 2, 4), affecting 0.5%-3% of women at the reproductive age (5). Due to multiple and complex diseases, in 50%-60% of RSA patients, the causative agent cannot be identified except the known causes, such as abnormal reproductive tract junction, reproductive tract inflammation, chromosomal abnormalities, endocrine disorders, immune dysfunction, pre-thrombotic state, etc. (5). Clinical studies (6)have found that the risk of spontaneous abortion in the next pregnancy in such patients is as high as

70% ~ 80%, which seriously affects the patients' physical and mental health. Due to complex causes involved in pregnancy loss and few evidence-based diagnostic strategies, RSA's etiology remains unexplained in more than half of those affected (7). Unfortunately, in 50% of the cases, RSA's cause remains unknown, and that group is defined as unexplained RSA.

RSA belongs to the categories of "slip pregnancy", "multiple abortions" and "repeated pregnancy abortion" in Traditional Chinese medicine. The treatment is advocated to use invigorating qi and kidney, clearing heat, and pacifying fetus. Some doctors believe that RSA should be used at the same time to promote blood circulation, blood stasis is closely related to fetal slip, and blood stasis is the pathological product of kidney deficiency. After the repeated abortion, kidney qi deficiency, blood circulation in the cytoskeleton is not smooth, fetal yuan loss and nourishment leads to abortion.

Traditional Chinese medicine (TCM) has been widely used in China for thousands of years. Chinese herbal medicine (CHM) has become a treatment option in many cancer centers in Asia, Western countries, and Africa (8–10).

Chinese herbal formulae always contain many kinds of herbs and could affect many targets, so herbal formulae's mechanisms are hard to understand. Network pharmacology, first proposed by Andrew L Hopkins (11), brings the hope to study the effective constituents and targets of herbs in a traditional Chinese formula, is to explore the relationship between drugs and diseases on the whole and explain the "multi-component, multi-target and multi-approach" pharmacological mechanism of single drugs or compound drugs, which is not compatible with the holistic concept of Traditional Chinese medicine (12). It has made significant pharmacology research achievements, new drug discovery, drug repositioning, and other aspects.

The traditional Chinese medicine systems pharmacology database and analysis platform (TCMSP) as a digital repository of traditional medicines. It can predict pharmacological targets and specific maladies of every dynamic compound and is a primary analytical tool in network pharmacology that helps determine the complex interactions between drugs and targets (13). Network pharmacology has helped elucidate several TCM formulations' mechanism so far (14, 15). As a result, the various public availability of network pharmacology platforms and other bioinformation databases (16) enable us to put TCMs-based drug discovery strategy into practice.

In this study, we used the network pharmacology approach to explore Bushen Huoxue Decoction (BHD) 's potential mechanism in treating RSA. We first filtered the TCMSP database for BHD's active compounds and identified the targets, followed by mining for disease-related genes and network analysis of those genes.

2 Materials And Methods

2.1 RSA significant genes collection

RSA significant genes were collected from 3 databases, TTD (http://db.idrblab.net/ttd/) (17), Drugbank (https://www.drugbank.ca/) (18) and DisGeNET (https://www.disgenet.org/) (19). The database was searched using the keyword 'recurrent spontaneous abortion' and 'spontaneous abortion', which yielded 125 known RSA-related genes of Homo sapiens. The repeated genes between the two databases were removed. To normalize the gene information, different ID types were converted to Uniprot (http://www.uniprot.org/) (20)[20]).

2.2 Chemical Components of Each representative Herb in BHD

To screen the active ingredients of BHD, we used the TCMSP database (http://tcmspw.com/tcmsp.php) (13). TCMSP is a unique systems pharmacology platform designed explicitly for Chinese medicine that contains information on their ADME characteristics and captures the relationships between disease, targets, ingredients, and drugs (21).

2.3 Pharmacokinetic Prediction of BHD

The chemical ingredients were collected from TCMSP Database (13). The ingredients were screened according to oral bioavailability (OB) and drug-likeness (DL) values. Specifically, the ingredients in the BHD meeting the criteria of OB $\geq$ 30% and DL $\geq$ 0.18 were chosen as candidate ingredients for further analysis.

OB refers to the percentage and rate of the release and absorption of active ingredients into the systemic blood circulation and is an essential pharmacokinetic index of oral drugs (22). It is also an important index to objectively evaluate the intrinsic quality of oral medications (23), particularly in the drug administration of most oral Chinese herbal formulas (24). DL is defined as a tricky balance of structural features and various molecular properties, determining whether the particular molecule is similar to the known drugs (23). These parameters, such as hydrogen bonding characteristics and hydrophobicity, mainly influence molecules' behavior in living organisms, which ultimately affects their transport properties, an affinity for proteins, metabolic stability, and many other properties.

2.4 Potential Targets of the Chemical Components of Bushen Huoxue method

We chose the TCMSP database as the primary source of component-target data and obtained each herb's target protein names in BHD. Only the proteins that had interactions with the bioactive components in BHD we had already obtained were selected. Then, we converted the target protein names of the bioactive components of BHD into gene names with the species limited into "Homo sapiens" with the UniProt Knowledgebase (UniProtKB, http:// www.uniprot.org) (25).

Target fishing was performed to search for or predict the potential targets of small molecules. The validated targets were extracted from SwissTargetPrediction (http://www.swisstargetprediction.ch/) (26).

The predicted targets were obtained using PubChem (https://pubchem.ncbi.nlm.nih.gov/) (27), an online tool for predicting targets based on 3D similarity.

2.5 RSA-BHD gene network establishment

To illustrate the possible interaction between RSA-related targets and the potential targets of BHD, we intersected the potential targets of BHD and RSA-related drug targets. We obtained the intersecting targets with Venn Diagram (http://bioinformatics.psb.ugent.be/webtools/Venn/). The overlapping target proteins of RSA and BHD were used to construct a protein-protein interaction (PPI) network with multiple protein patterns on the Search Tool for the Retrieval of Interacting Genes/Proteins (STRING) platform (https:// string-db.org/, version 11.0). We set the organism type to "Homo sapiens" and left the default settings in place for the other parameters. Then, we exported the downloaded "string_interactions.tsv" file and imported it into Cytoscape 3.8.2 to obtain the PPI network and perform network analysis. In the network, nodes represent the target proteins, and edges represent the interaction between proteins.

The ingredients-targets networks were constructed for these herbs using Cytoscape software46 (Version 3.8.2). The networks were analyzed using Cytoscape to calculate topological parameters, including the degree, betweenness, closeness and centroid. The significant nodes representing putative major ingredients and major targets of herbs were explored.

2.6 GO and KEGG Pathway Enrichment Analysis

Gene Ontology (GO, http://www.geneontology.org/) and Kyoto Encyclopedia of Genes and Genomes (KEGG, http://www.genome.jp/kegg/) pathway analysis were used to analyze the primary pharmacological units. GO is a database that functionally annotates genes and proteins into three main terms-cellular components (CC), molecular functions (MF), and biological processes (BP) (28) and pathway analysis reveals the possible biological processes with essential hub genes. KEGG is a database for determining the high-level functions and biological relevance of a large set of genes (29). The molecular action of the mechanism of BHD could be elucidated by analyzing the significant GO terms and pathways of the overlapping genes. The Cytoscape and RStudio 4.0.2 (ggplot2) were used to integrate the GO terms with KEGG pathways (30). We selected the standard *P*-value cutoff of 0.05 and performed the enrichment analysis.

2.7 Experimental validation

2.7.1 Preparation of BHD water extract

Radix Salviae, *Chuanxiong Rhizoma*, *Cuscutae Semen* and *Eucommiae Cortex* were into powder. A total of 40 g powder was weighed and soaked in water for 12 h at 4℃. BHD aqueous solution was boiled to 100 ml, that is, the concentration of BHD water extract reached 40 mg/mL, and BHD crude water extract was obtained through rough filtration through 3 layers of sterile nylon mesh with an aperture of 0.15 mm. BHD crude water extract was isolated for 10 min at 1200 g, the supernatant was collected, and then

filtered with 0.22 μm filter membrane to obtain the mother liquor of BHD water extract, which was stored at -20℃ for standby use.

2.7.2 Cell culture, Reagents and antibodies

HTR-8/SVneo cells (provided by Dr. Charles Graham, Queen's University of Canada) at the logarithmic growth stage were cultured in a 37°C, 5% CO_2 incubator plated on a six-well culture plate at a density of 1 × 10^5 cells per well. After 24 hours, H_2O_2 (Sigma-Aldrich, USA) was added at concentrations of 300 μmol/L and 3hours to the culture to establish an oxidative stress model of HTR-8/SVneo cells (Model). Cells in the experimental group were incubated with gradient diluted BHD water extracts (1 mg/mL, 5 mg/mL, 10 mg/mL, 20 mg/mL) for 48 h, and cells without any treatment were used as the control group (Control). The morphology of the cells was observed under an inverted microscope.

PTGFR was obtained from Abcam (Cambridge, UK), and other antibodies were obtained from Proteintech (Chicago, USA). PTGFR (ab126709, 1:2000), AGTR1(25343-1-AP, 1:500), OXTR (23045-1-AP, 1:1000), GAPDH (10494-1-AP, 1:5000).

2.7.3 Cell activity assay by CCK-8

After the culturing period had elapsed, the culture supernatant was removed and washed twice with PBS. Then 110 μL of CCK-8 working solution was added (prepared in advance at a volume ratio of CCK-8 solution to culture medium of 1:10). This mixture was incubated in 37°C for 2 hours, and then the absorbance (expressed as the optical density [OD]) value of each well at 450 nm was detected using an automatic enzyme scale. The cell survival rate was calculated using the following formula: survival rate (%) = (experiment-group OD – blank-pore OD) / (control-group OD – blank pore OD) × 100%.

2.7.4 Western blot

Cultured cells were harvested with a rubber scraper and washed twice with cold phosphate-buffered saline (PBS). Cell pellets were lysed and kept on ice for at least 20 min in RIPA lysis buffer (Millipore), with phenylmethylsulphonyl fluoride and protease inhibitors cocktail (Thermo Scientific). The lysates were cleared by centrifugation, and the supernatants were collected. The BCA assay quantified proteins, and loading buffer 5X was added to the proteins which were incubated for 5 min at 95 °C. Then, proteins were loaded on an SDS-PAGE polyacrylamide gel, transferred to Immobilon-P PVDF membrane (Millipore), probed with the appropriate primary antibodies, and detected by chemiluminescence (ECL, Thermo Scientific). Images were then acquired with an Image-Lab software (Bio-Rad). Image analysis of western blots was performed with Image-Lab analyzer software.

2.7.5 Quantitative real-time polymerase chain reaction (qRT-PCR)

According to the manufacturer's instructions, total RNA was extracted from cell cultures using TRIzol® (Life Technologies, Carlsbad, CA). RNA (1 μg) was reverse transcribed to cDNA templates using iScript cDNA synthesis kit (Bio-Rad, Hercules, CA). For semiquantitative RT-PCR, cDNA (25 ng) was amplified

using SYBR® Green PCR Master Mix (Life Technologies) and oligonucleotide primers for specific target sequences on an Applied Biosystems 7500 Real-Time PCR system. RT-PCR parameters were as follows: denaturating at 95 °C for 10 min, followed by 40 cycles of denaturing at 95 °C for 15 s and annealing/extension at 60 °C for 60 s. The system software automatically calculated threshold cycles (Ct). The expression of GAPDH normalized the expression level of the target mRNA. The collected data were quantified using the $2^{-\Delta\Delta Ct}$ method. Primer sequences are listed:

Homo PTGFR:

Forward: 5'- CTGTGGAGTGCATGTCATC – 3'

Reverse: 5'- GGTGACTCAGAAATAGCAGCAA – 3'

Homo AGTR1:

Forward: 5'- AACAGCTTGGTGGTGATCGTC – 3'

Reverse: 5'- -CATAGCGGTATAGACAGCCCA – 3'

Homo OXTR:

Forward: 5'- TGCTACGGCCTTATCAGCTT – 3'

Reverse: 5'- CTCCACATCTGCACGAAGAA – 3'

Homo GAPDH:

Forward: 5'-GCCATCACTGCCACCCAG-3

Reverse: 5'-TCTTACTCCTTGGAGGCCATGT-3'

2.7.6 Statistical analysis

All data are expressed as mean ± SD, obtained from more than three independent experiments, and analyzed by GraphPad Prism 8.0 (GraphPad Software, CA, USA). Statistically significant differences (*P< 0.05, **P< 0.01) were examined using the Student's t-test and one-way ANOVA.

3 Result

3.1 RSA-Related Target Network

The RSA is a complex polygenic, multifactorial disorder. This study obtained 125 targets related to PCOS through the TTD database, Drugbank database, and DisGeNET database.

3.2 Chemical Ingredients of BHD

A total of 76 chemical ingredients passed the filters of OB ≥ 30% and DL ≥ 0.18 of the four herb medicines were retrieved from TCMSP, including 43 ingredients in *Radix Salviae*, 3 ingredients in *Chuanxiong Rhizoma*, 10 ingredients in *Cuscutae Semen*, and 20 ingredients in *Eucommiae Cortex*. Remove all duplicates, the pharmacokinetic properties of the 73 ingredients are shown in Table 1.

Table 1
Active compounds properties

Latin name	Molecule Name	OB (%)	DL
Radix Salviae	Poriferasterol	43.83	0.76
Chuanxiong Rhizoma	poriferast-5-en-3beta-ol	36.91	0.75
Cuscutae Semen	isoimperatorin	45.46	0.23
Eucommiae Cortex	sugiol	36.11	0.28
	Dehydrotanshinone II A	43.76	0.4
	Baicalin	40.12	0.75
	digallate	61.85	0.26
	luteolin	36.16	0.25
	α-amyrin	39.51	0.76
	5,6-dihydroxy-7-isopropyl-1,1-dimethyl-2,3-dihydrophenanthren-4	33.77	0.29
	2-isopropyl-8-methylphenanthrene-3,4-dione	40.86	0.23
	3α-hydroxytanshinone□a	44.93	0.44
	(E)-3-[2-(3,4-dihydroxyphenyl)-7-hydroxy-benzofuran-4-yl]	48.24	0.31
	4-methylenemiltirone	34.35	0.23
	2-(4-hydroxy-3-methoxyphenyl)-5-(3-hydroxypropyl)-7-methoxy	62.78	0.4
	6-o-syringyl-8-o-acetyl shanzhiside methyl ester	46.69	0.71
	formyltanshinone	73.44	0.42
	3-beta-Hydroxymethyllenetanshiquinone	32.16	0.41
	Methylenetanshinquinone	37.07	0.36
	przewalskin a	37.11	0.65
	przewalskin b	110.32	0.44
	Przewaquinone B	62.24	0.41
	przewaquinone c	55.74	0.4
	(6S,7R)-6,7-dihydroxy-1,6-dimethyl-8,9-dihydro-7H-naphtho	41.31	0.45
	sclareol	40.31	0.46
	tanshinaldehyde	43.67	0.21
	Danshenol B	52.47	0.45
		57.95	0.56

Latin name	Molecule Name	OB (%)	DL
	Danshenol A	56.97	0.52
	Salvilenone	30.38	0.38
	cryptotanshinone	52.34	0.4
	dan-shexinkum d	38.88	0.55
	danshenspiroketallactone	50.43	0.31
	deoxyneocryptotanshinone	49.4	0.29
	dihydrotanshinlactone	38.68	0.32
	dihydrotanshinone□	45.04	0.36
	epidanshenspiroketallactone	68.27	0.31
	C09092	36.07	0.25
	isocryptotanshi-none	54.98	0.39
	Isotanshinone II	49.92	0.4
	manool	45.04	0.2
	microstegiol	39.61	0.28
	miltionone □	49.68	0.32
	miltionone □	71.03	0.44
	miltipolone	36.56	0.37
	Miltirone	38.76	0.25
	miltirone □	44.95	0.24
	neocryptotanshinone ii	39.46	0.23
	neocryptotanshinone	52.49	0.32
	1-methyl-8,9-dihydro-7H-naphtho[5,6-g]benzofuran-6,10,11	34.72	0.37
	prolithospermic acid	64.37	0.31
	(2R)-3-(3,4-dihydroxyphenyl)-2-[(Z)-3-(3,4-dihydroxyphenyl)acryloyl]	109.38	0.35
		88.54	0.26
	(Z)-3-[2-[(E)-2-(3,4-dihydroxyphenyl)vinyl]-3,4-dihydroxy-phenyl]	45.56	0.61
	salvianolic acid g	43.38	0.72
	salvianolic acid j	32.43	0.23
	salvilenone □	31.72	0.24

Latin name	Molecule Name	OB (%)	DL
	salviolone	34.49	0.28
	NSC 122421	42.67	0.45
	Tanshindiol B	42.85	0.45
	Przewaquinone E	49.89	0.4
	tanshinone iia	65.26	0.45
	(6S)-6-(hydroxymethyl)-1,6-dimethyl-8,9-dihydro-7H	45.64	0.3
	tanshinone □	42	0.19
	Mandenol	65.95	0.27
	Perlolyrine	47.66	0.24
	senkyunone	36.91	0.75
	sitosterol	56.55	0.83
	sesamin	39.25	0.76
	NSC63551	49.6	0.31
	isorhamnetin	36.91	0.75
	beta-sitosterol	41.88	0.24
	kaempferol	37.58	0.71
	campest-5-en-3beta-ol	43.78	0.76
	Isofucosterol	63.77	0.25
	matrine	37.87	0.68
	CLR	46.43	0.28
	Quercetin	57.2	0.62
	40957-99-1	55.38	0.78
	Mairin	36.91	0.75
	beta-sitosterol	41.88	0.24
	kaempferol	49.18	0.55
	Erythraline	43.35	0.77
	Acanthoside B	92.43	0.55
	AIDS214634	32.16	0.41
	3-beta-Hydroxymethyllenetanshiquinone	48.96	0.24

Latin name	Molecule Name	OB (%)	DL
	ent-Epicatechin	57.53	0.81
	Yangambin	30.51	0.85
	Eucommin A	87.19	0.62
	(+)-medioresinol	58.67	0.61
	(-)-Tabernemontanine	55.42	0.82
	Cyclopamine	30.1	0.24
	Dehydrodieugenol	68.22	0.4
	Cinchonan-9-al, 6'-methoxy-, (9R)-	45.58	0.83
	GBGB	77.01	0.19
	Helenalin	33.29	0.62
	(+)-Eudesmin	50.76	0.39
	4-[(2S,3R)-5-[(E)-3-hydroxyprop-1-enyl]-7-methoxy-3-methylol	46.43	0.28
	quercetin	37.18	0.58
	beta-carotene	56.32	0.36
	(E)-3-[4-[(1R,2R)-2-hydroxy-2-(4-hydroxy-3-methoxy-phenyl)-1	36.82	0.37
	Syringetin		

3.3 Putative major ingredients and major targets of BHD

A total of 6682 potential targets from the 73 ingredients were retrieved from the TCMSP database. After eliminating the overlapping proteins, 1084 related proteins were obtained and converted into gene names with the species limited into "Homo sapiens" based on the UniProtKB.

Ingredient-target networks were constructed for the 4 herbs (Fig. 3). The major putative ingredients and targets of each herb were listed in Table 2.

Table 2
The putative major ingredients and major targets of 4 herbs

Latin name	Number of ingredients	Major ingredients	Major targets
Radix Salviae	43	Dehydrotanshinone II A	ACHE
Chuanxiong Rhizoma	3	Methylenetanshinquinone	HSD11B1
Cuscutae Semen	10	Danshenol A	AKR1B1
Eucommiae Cortex	20	Cryptotanshinone	CYP19A1
		tanshinone iia	ADORA2A
		Mandenol	SRC
		Sitosterol	MTNR1B
		campest-5-en-3beta-ol	MTNR1A
		beta-sitosterol	NPY5R
		Isofucosterol	ESR2
		CLR	PLA2G1B
		40957-99-1	AKR1B10
		(+)-medioresinol	CYP19A1
		Syringetin	ADORA2A
		quercetin	PIM1
		kaempferol	CDK2
			EGFR
			CDK1

Figure 1(A) shows that the *Radix Salviae* network consisted of 918 nodes and 4300 edges, containing 875 predicted targets. The network analysis revealed that beta-sitosterol (1 validated target, 59 predicted targets) was predicted as the major ingredient in *Radix Salviae*. Genes such as ESR1, KRAS, and PTGS2 were predicted as the major targets of RST for the Treatment of HCC. As shown in Fig. 1(B), the *Chuanxiong Rhizoma* network consisted of 245 nodes, 300 edges, including 242 predicted targets. Among the ingredients of *Chuanxiong Rhizoma*, beta-sitosterol was also predicted as a major ingredient. Genes such as ESR1, KRAS, and AURKA were predicted as major targets of FC for the Treatment of HCC. The *Cuscutae Semen* network consisted of 410 nodes, 1000 edges, and contained 400 predicted targets (Fig. 1(C)). Galacturonic acid (0 validated targets, 52 predicted targets) was predicted as the major ingredient of *Cuscutae Semen* for the Treatment of RSA, and ASS1, GSTP1, and NOS2A were predicted as the major targets of CT. The *Eucommiae Cortex* network consisted of 758 nodes, 1982 edges, including

738 predicted targets (Fig. 1(D)). Beta-sitosterol was also the major ingredient, and genes such as KRAS, CCNA2, and ESR1 were predicted as major targets of *Eucommiae Cortex* for RSA's treatment.

As shown in Table 2, although many ingredients may contribute to herbs' RSA treatment effects, researching the major ingredients is a practical approach to elucidate the pharmacological mechanisms of herbs' action. In this study, network pharmacology was applied to explore the major ingredients.

3.4 Network analysis

Among the above 125 RSA-related targets, BHD shared 26 common targets with RSA (Fig. 2). The 26 putative therapeutic targets were imported into the STRING database to establish the putative therapeutic target PPI network. The "string_interaction.tsv" file was then imported into Cytoscape 3.8.2 to perform network analysis. The network had 26 nodes, which interacted with 24 edges. The average node degree is 1.85, and the average local clustering coefficient is 0.544.

In such a network, a node can represent a herb, a compound, or a gene/protein, and an "edge" is an association between the nodes. The "degree" of a hub is the number of edges associated with it, and the "betweenness" of a hub is the number of closest associations. The nodes whose connectivity was more significant than twice the median of all nodes are selected as the network's hub nodes. The hubs with high centrality are considered the key hubs in a network. From yellow to green in our network, the degrees of freedom increase suggest stronger interactions (Fig. 3). These results demonstrate that these targets are closely related to others in the network and may play key roles in RSA. The targets of 26 putative therapeutic targets in the Treatment of RSA include HSD17B1, MMP7, PREP, OXTR, PTGFR, AHR, DHFR, HSD3B1, JAK2, F2, TGFBR1, AGTR1, PTGIR, MMP12, F13A1, PTGER2, RBP4, MGAT2, LGALS3, MAP2, CHIA, GLS, IL1B, IGFBP3, CYP24A1, and DRD1. Our results indicated that the top mutual target proteins have various beneficial functions for treating RSA at the molecular level.

3.5 GO Functional Enrichment Analysis

GO functions of the RSA specific drug targets were annotated to clarify the mechanism of action of BHD in RSA. GO enrichment analysis was performed on the 26 targets using DAVID database (https://david.ncifcrf.gov/) and RStudio (ggplot2). The most enriched terms in GO analysis are shown in Figs. 4.

In detail, and the top 10 BP terms were mainly enriched in elevation of cytosolic calcium ion concentration; cytosolic calcium ion homeostasis; positive regulation of transport; cellular calcium ion homeostasis; calcium ion homeostasis; cellular metal ion homeostasis; metal ion homeostasis; cellular di-, tri-valent inorganic cation homeostasis; regulation of cell proliferation; di-, tri-valent inorganic cation homeostasis.

The top 10 CC terms were mainly enriched in extracellular region part; extracellular space; integral to plasma membrane; intrinsic to plasma membrane; extracellular region; cell fraction; membrane fraction; insoluble fraction; plasma membrane part; caveola.

And the top 10 MF terms were prostaglandin receptor activity; icosanoid receptor activity; prostanoid receptor activity; endopeptidase activity; steroid dehydrogenase activity, acting on the CH-OH group of donors, NAD or NADP as acceptor; sugar binding; peptide binding; steroid dehydrogenase activity; peptidase activity, acting on L-amino acid peptides; peptidase activity.

3.6 KEGG pathway Analysis

To clarify these targets' biological actions, we performed KEGG analysis and pathway enrichment analysis with the DAVID database and RStudio (ggplot2) database. We listed the genes of major RSA putative therapeutic targets. We imported them into RStudio to generate relevant pathways that might have an essential influence on the biological process of BHD in treating RSA. Pathways with an adjusted *P*-value < 0.05 were considered significant.

A total of 19 signaling pathways were significantly enriched through pathway enrichment analysis. In the bubble diagram (Fig. 5), the nodes' color and size were determined according to the related genes' numbers and *P*-values. The color from pink to purple reflects the adjusted *P*-values from large to small, and the node size indicates the number of related genes. The bubble chart was separately arranged according to the *P*-value and the number of related genes.

According to the *P*-value, the Neuroactive ligand-receptor interaction;Th17 cell differentiation; AGE-RAGE signaling pathway in diabetic complications; Calcium signaling pathway; Renin-angiotensin system; Metabolic pathways; Antifolate resistance; Cushing's syndrome; cAMP signaling pathway; Ovarian steroidogenesis were within the top 10 terms.

According to the number of related genes, Neuroactive ligand-receptor interaction; Metabolic pathways; Th17 cell differentiation; AGE-RAGE signaling pathway in diabetic complications; Calcium signaling pathway; Pathways in cancer; Cushing's syndrome; cAMP signaling pathway; Renin-angiotensin system; Antifolate resistance were in the top 10 terms.

The overlapping terms of the above lists included the Neuroactive ligand-receptor interaction; Metabolic pathways; Th17 cell differentiation; AGE-RAGE signaling pathway in diabetic complications; Calcium signaling pathway; cAMP signaling pathway.

3.7 CCK-8 assay was used to detect the optimal adaptive concentration activity of BHD on HTR-8/SVneo cell oxidative stress model

As shown in Fig. 6B, the cell survival rate of HTR-8/SVneo cells after treatment with BHD by CCK-8, the experimental group was over 80% in the BHD water extract concentration of 1 mg/mL and 5 mg /mL after 48 h ($P < 0.01$). Observed according to Fig. 1 the results showed that different concentrations of extracts from BHD and cell incubation culture after 48 h, Control group has no obvious change, and add 10 mg/mL, 20 mg/mL BHD water extract of experimental group cells appear obvious morphological changes and pathological changes, including cells, shrinkage, it becomes off from cell culture on the

surface, etc. (Fig. 6A). Combine the two results, 5 mg/mL was taken as the maximum safe working concentration of BHD water extract.

3.8 BHD participated in the treatment of RSA through the pathway

To investigate whether our previous bioinformatics results are correct. According to the results of KEGG, Neuroactive ligand-receptor interaction pathway was selected for verification, and genes enriched in this pathway were selected We verified whether BHD has a certain therapeutic effect on RSA. The western blot results (Fig. 6C, Fig. 7DEF) showed that the expression of PTGFR, AGTR1 and OXTR were significantly increased in the Model group rather than the Control group ($P < 0.05$). And the experimental group (5 mg/mL) rather than Model group ($P < 0.05$). Meanwhile, to confirm the results of western blotting in the cells, qRT-PCR analysis of BHD water extract in RSA treatment is shown in Fig. 7ABC. The results of PTGFR, AGTR1 and OXTR genes expression detected by qRT-PCR showed that the expression level of PTGFR, AGTR1 and OXTR genes were significantly decreased compared with the model group when the water extract (5 mg/mL) with a safe concentration gradient was added to the cells in the experimental group ($P < 0.05$).

4 Discussion

TCM, consists of complex formulations that have hitherto been difficult to characterize, thus limiting their widespread clinical use, the disease name of RSA is "slippery fetus" and "multiple abortions", which also belong to the category of "repeated pregnancy and repeated abortion", which refers to abortion or miscarriage occurring for 3 consecutive times or more (31). TCM has a long history in treating menstrual diseases and infertility and has achieved sound effects (32). TCM advocates the principles of pre-cultivation, prevention before pregnancy, survival without death, and prevention of pregnancy and change. The method of tonifying kidney, activating blood circulation and removing blood stasis has been used to treat slippery fetus since ancient times. Recent studies have shown that kidney deficiency and blood stasis are the primary syndrome type of recurrent flow induced by pre-thrombotic and unknown causes. Although Huo Xue drugs are contradictions for pregnancy, they follow the treatment principle of "there was a cause without a disappearance, nor a disappearance, and most of them were lost" in < Suwen · Liuyuan Zhengji Grand Essay >. The doctors should not be prejudiced-out and cautious. The method of Bushen Huoxue can achieve a good curative effect in the treatment of recurrent abortion.

In this study, several network pharmacology-based methods were used to predict potential targets. This approach provides new clues to exploring ethnopharmacology and herbal or even TCM formulas. By analyzing the putative therapeutic target network and biological functions by GO and KEGG function enrichment, the potential pharmacological and molecular mechanisms of BHD in treating RSA were preliminary revealed.

The drug-target network and the RSA network had 26 overlapping genes, were enriched in 19 pathways, and are likely the key pathway involved in RSA treatment. According to the *P*-value and Ration of KEGG pathway enrichment, we hypothesized that BHD plays a role in tonifying kidney and activating blood stasis by regulating the Neuroactive ligand-receptor interaction. Therefore, we conducted a series of experiments to confirm that BHD participates in this pathway during the treatment of RSA.

Neuroactive steroids are hormones that act as regulators of neurotransmitter receptors to either enhance or suppress neuronal activity. The effect of steroid exhibits marked stereoselectivity, suggesting a ligand-receptor interaction. According to the literature, neuroactive steroid influences the modulation of fetal neurodevelopment (33). Neuroactive ligands affect neuronal function by binding to intracellular receptors, which can bind transcription factors (34). The number of apoptotic cells in the brain and central nervous system of zebrafish embryos was increased in the expression of genes involved in the neuroactive ligand-receptor interaction pathway (35). Based on these, we infer that BHD might serve a crucial role in human reproduction by influencing the pathway of Neuroactive ligand-receptor interaction.

HTR-8/SVneo cell line is considered the closest study model to trophoblast cells derived from early human pregnancy (8 ~ 10 weeks) (36). The HTR-8/SVneo human trophoblast cell line applied in the present study is more similar to primary trophoblasts and normal human physiological conditions. Our previous study showed that the H_2O_2 treatment of HTR-8/SVneo cells could establish a placental oxidative stress model and simulate the mechanism of recurrent abortion in vitro (37).

A total of 26 genes were screened out by PPI network, among which 7 were enriched in this pathway, 3 of which were selected for experimental verification. Firstly, the safe drug concentration of BHD on cells was screened out by cell morphology and cell activity by CCK-8 assay. The results showed that the cell model of oxidative stress at the 5 mg/mL BHD water extract concentration could approach control cells.

PGF2α receptor (PTGFR), produced by the myometrium and intrauterine tissues of pregnancy, involves five distinct yet integrated physiological events: the rupture of the membranes, cervical ripening and dilatation, contractility of the myometrium, placental separation and uterine involution (38).

PTGFR is an essential uterine activation protein (UAP), promoting the tissues' ability to carry out the process of parturition. Myometrial PTGFR mRNA is elevated at term and preterm birth in humans and rodents (39, 40). Also, infusion of a specific inhibitor, THG113.31, in sheep and mice delays preterm birth and prolongs gestation (41, 42). In rats, myometrial PTGFR mRNA expression rate decreases during pregnancy, and its expression increases significantly again at term (43). We added 5 mg/mL BHD into the cell model of RSA oxidative stress. Western blot results showed that the expression level of PTGFR protein was significantly decreased compared with that of the model group.

Meanwhile, at the RNA level, qRT-PCR results were the same as western blot results. Our results are consistent with previous reports and network pharmacologic results. This suggests that PTGFR plays a central role in both pregnancy maintenance and parturition. PTGFR may act via its receptor to amplify the direct actions of cytokines. Together, these feed-forward mechanisms activate the uterus, trigger uterine

contractile stimulants' production, and lead to labor and delivery (44). We suggest that the role of the PTGFR in the human uterus requires further validation prior to pursuing it as a target for RSA treatment.

Angiotensin II type I receptor (AGTR1), a component of the renin-angiotensin system (RAS). AGTR1 encodes the angiotensin II (Ang II) type I receptor belonging to the family of G-protein coupled receptors (45). AGTR1 is a major effector controlling blood pressure in the cardiovascular system and induces diverse signal transduction pathways (46). It regulates the aldosterone secretion and is involved in vascular remodeling, inflammation and endothelial dysfunction (47). We found that AGTR1 gene expression was significantly higher in HTR-8/SVneo oxidative stress cell models than in normal cells, both at protein and RNA levels. Alterations in the maternal renin-angiotensin system (RAS) (48) have been implicated in the pathogenesis of RSA (49, 50). The RAS plays a crucial role in maintaining a normal pregnancy, where plasma levels of renin, angiotensin II, and aldosterone are up-regulated (51). Angiotensin II is the primary signaling molecule of the RAS and its major cardiovascular effects are mediated by angiotensin II receptor type 1 (gene denoted as AGTR1), including vasoconstriction, vascular growth promotion, anti-natriuresis, aldosterone synthesis, and inhibition of renin synthesis and release (52). In RSA, this equilibrium is disrupted, and these proteins' plasma levels decrease toward the normal non-gravid range. The TCM decoction BHD can correct this imbalance. After the addition of a safe concentration of BHD, the expression level of AGTR1 protein in cells was significantly decreased. In addition, the AGTR1 level in RNA was lower compared to the model group. Any imbalance results in a pathological state. These results suggest that BHD altered AGTR1 and RSA's imbalance to reach new homeostasis, which was more suitable for a normal pregnancy.

The oxytocin receptor (OXTR) gene is a protein that works as a receptor for the widely expressed oxytocin, which acts both as a hormone and neurotransmitter.

Studies (53–56) have shown that a decrease in the progesterone level coupled with the activation of OXTR leads to intense inflammation, transforming the uterus from the quiescent state to the activated state and resulting in premature labor or abortion. We found that in the cell model of oxidative stress, the expression level of OXTR was significantly increased compared with the normal cell group, which was consistent with the previous research results and proved that this gene was one of the critical reasons for the development of RSA. OXTR, an important inflammatory factor, plays a vital role in initiating and maintaining delivery (57, 58). Myometrium and decidua from pregnant women who underwent cesarean section or hysterectomy during pregnancy (59), and the results showed that OXTR level was low in early pregnancy, whereas in pregnant women with at least 37-week gestational age or premature labor, OXTR level and the sensitivity to oxytocin were significantly higher. In pregnant women with prolonged pregnancy (> 42-week gestational age), the OXTR level was significantly lower. The mRNA level of OXTR is related to premature labor. Further, progesterone and its receptor directly inhibit the mRNA level of OXTR, thus preventing premature labor (60). Our experimental results showed that BHD had the same effect as progesterone and could significantly reduce the expression of elevated OXTR protein and RNA in the oxidative stress model cells. Mammalian animal studies have shown that the balance between progesterone and its receptor plays a critical role in maintaining normal pregnancy (61); other studies

have shown that progesterone maintains uterus stability by inhibiting OXTR (62). These results indicate that OXTR plays a vital role in pregnancy and delivery and TCM can achieve progesterone very well.

5 Conclusion

In conclusion, TCM treatment was associated with a survival benefit in patients with RSA. Besides, the use of the network pharmacology method helps explore the underlying treating RSA mechanisms of herbs by predicting active ingredients and molecular targets of herbs. Combined with network pharmacology and experimental verification, it fully demonstrates that TCM can play a dominant role in RSA treatment. These roles may be realized by reducing the expression of PTGFR, AGTR1 and OXTR genes through the Neuroactive ligand-receptor interaction pathway. In this study, the combination of clinical research and network pharmacology is a promising research method for the "precise treatment of TCM" was proved through the validation of cell experiments. A complete understanding of key players in regulating the molecular processes leading to parturition will have significant consequences to human health.

Abbreviations

BHD Bushen Huoxue Decoction

RSA recurrent spontaneous abortion

TCM Traditional Chinese medicine

CHM Chinese herbal medicine

TCMSP The traditional Chinese medicine systems pharmacology database and analysis platform

PPI protein-protein interaction

STRING Search Tool for the Retrieval of Interacting Genes/Proteins

GO Gene Ontology

CC cellular components

MF molecular functions

BP biological processes

KEGG Kyoto Encyclopedia of Genes and Genomes

PBS phosphate-buffered saline

PTGFR PGF2α receptor

AGTR1 Angiotensin II type I receptor

OXTR The oxytocin receptor

Declarations

Funding: This work is supported financially by the National Natural Science Foundation of China (NSFC) No. 81703797 and the National Administration of Traditional Chinese Medicine Project.

Ethics approval and consent to participate: Not applicable.

Competing Interest: The authors declare that they have no conflict of interest.

Consent for publication: Not applicable.

Availability of data and material: All data generated or analyzed during this study are available from the corresponding author on reasonable request.

Acknowledgments: This work is supported financially by the National Natural Science Foundation of China (NSFC) No. 81703797 and is the National Administration of Traditional Chinese Medicine Project.

Author contributions：All authors read and edited several draft versions and all approved the final manuscript.

LI Meihe, WU Jinping: Conceptualization, Data curation, Writing- Original draft preparation. KANG Minchao, YING Xu: Methodology, Software. DANG Huimin: Visualization, Investigation. XU Xin: Supervision, Writing-Reviewing and Editing

Contributor Information:

LI Meihe, Email: limeihe.md@gmail.com

WU Jinping, Email: 3296538566@qq.com

KANG Minchao, Email: kagminchao@stu.xjtu.edu.cn

XU Ying, Email: xjtuxuyingying@126.com

DANG Huimin, Email: wbb.23@163.com

XU Xin, Email: xuxindoudou1959@163.com

References

1. Salat-Baroux J. [Recurrent spontaneous abortions]. Reprod Nutr Dev. 1988;28(6b):1555–68.

2. Definitions of infertility. and recurrent pregnancy loss: a committee opinion. Fertil Steril. 2013;99(1):63.10.1016/j.fertnstert.2012.09.023: 10.1016/j.fertnstert.2012.09.023.
3. Pereza N, Ostojić S, Kapović M, Peterlin B. Systematic review and meta-analysis of genetic association studies in idiopathic recurrent spontaneous abortion. Fertil Steril. 2017;107(1):150-9.e2.10.1016/j.fertnstert.2016.10.007: 10.1016/j.fertnstert.2016.10.007.
4. Grimstad F, Krieg S. Immunogenetic contributions to recurrent pregnancy loss. J Assist Reprod Genet. 2016;33(7):833–47.10.1007/s10815-016-0720-6: 10.1007/s10815-016-0720-6.
5. Branch DW, Gibson M, Silver RM. Clinical practice. Recurrent miscarriage. N Engl J Med. 2010;363(18):1740–7. 10.1056/NEJMcp1005330: 10.1056/NEJMcp1005330.
6. Hendriks E, MacNaughton H, MacKenzie MC. First Trimester Bleeding: Evaluation and Management. Am Fam Physician. 2019;99(3):166–74.
7. Gupta S, Agarwal A, Banerjee J, Alvarez JG. The role of oxidative stress in spontaneous abortion and recurrent pregnancy loss: a systematic review. Obstet Gynecol Surv. 2007;62(5):335–47; quiz 53 –4.10.1097/01.ogx.0000261644.89300.df: 10.1097/01.ogx.0000261644.89300.df.
8. Hyodo I, Amano N, Eguchi K, Narabayashi M, Imanishi J, Hirai M, et al. Nationwide survey on complementary and alternative medicine in cancer patients in Japan. J Clin Oncol. 2005;23(12):2645–54. 10.1200/jco.2005.04.126: 10.1200/jco.2005.04.126.
9. Evans MA, Shaw AR, Sharp DJ, Thompson EA, Falk S, Turton P, et al. Men with cancer: is their use of complementary and alternative medicine a response to needs unmet by conventional care? Eur J Cancer Care (Engl). 2007;16(6):517–25.10.1111/j.1365-2354.2007.00786.x: 10.1111/j.1365-2354.2007.00786.x.
10. Swarup AB, Barrett W, Jazieh AR. The use of complementary and alternative medicine by cancer patients undergoing radiation therapy. Am J Clin Oncol. 2006;29(5):468–73. 10.1097/01.coc.0000221326.64636.b2: 10.1097/01.coc.0000221326.64636.b2.
11. Hopkins AL. Network pharmacology: the next paradigm in drug discovery. Nat Chem Biol. 2008;4(11):682–90.10.1038/nchembio.118: 10.1038/nchembio.118.
12. Yang M, Chen JL, Xu LW, Ji G. Navigating traditional chinese medicine network pharmacology and computational tools. Evid Based Complement Alternat Med. 2013;2013:731969.10.1155/2013/731969: 10.1155/2013/731969.
13. Ru J, Li P, Wang J, Zhou W, Li B, Huang C, et al. TCMSP: a database of systems pharmacology for drug discovery from herbal medicines. J Cheminform. 2014;6:13.10.1186/1758-2946-6-13: 10.1186/1758-2946-6-13.
14. Wang S, Tong Y, Ng TB, Lao L, Lam JK, Zhang KY, et al. Network pharmacological identification of active compounds and potential actions of Erxian decoction in alleviating menopause-related symptoms. Chin Med. 2015;10:19.10.1186/s13020-015-0051-z: 10.1186/s13020-015-0051-z.
15. Wu L, Wang Y, Li Z, Zhang B, Cheng Y, Fan X. Identifying roles of "Jun-Chen-Zuo-Shi" component herbs of QiShenYiQi formula in treating acute myocardial ischemia by network pharmacology. Chin Med. 2014;9:24.10.1186/1749-8546-9-24: 10.1186/1749-8546-9-24.

16. Gao L, Wu WF, Dong L, Ren GL, Li HD, Yang Q, et al. Protocatechuic Aldehyde Attenuates Cisplatin-Induced Acute Kidney Injury by Suppressing Nox-Mediated Oxidative Stress and Renal Inflammation. Front Pharmacol. 2016;7:479.10.3389/fphar.2016.00479: 10.3389/fphar.2016.00479.
17. Wang Y, Zhang S, Li F, Zhou Y, Zhang Y, Wang Z, et al. Therapeutic target database 2020: enriched resource for facilitating research and early development of targeted therapeutics. Nucleic Acids Res. 2020;48(D1):D1031-d41.10.1093/nar/gkz981: 10.1093/nar/gkz981.
18. Wishart DS, Feunang YD, Guo AC, Lo EJ, Marcu A, Grant JR, et al. DrugBank 5.0: a major update to the DrugBank database for 2018. Nucleic Acids Res. 2018;46(D1):D1074-d82.10.1093/nar/gkx1037: 10.1093/nar/gkx1037.
19. Piñero J, Queralt-Rosinach N, Bravo À, Deu-Pons J, Bauer-Mehren A, Baron M, et al. DisGeNET: a discovery platform for the dynamical exploration of human diseases and their genes. Database. 2015;2015:bav028.10.1093/database/bav028: 10.1093/database/bav028.
20. UniProt. the universal protein knowledgebase. Nucleic Acids Res. 2017;45(D1):D158-d. 69.10.1093/nar/gkw1099: 10.1093/nar/gkw1099.
21. Lee WY, Lee CY, Kim YS, Kim CE. The Methodological Trends of Traditional Herbal Medicine Employing Network Pharmacology. Biomolecules. 2019;9(8).10.3390/biom9080362: 10.3390/biom9080362.
22. Fong SY, Bauer-Brandl A, Brandl M. Oral bioavailability enhancement through supersaturation: an update and meta-analysis. Expert Opin Drug Deliv. 2017;14(3):403–26. 10.1080/17425247.2016.1218465: 10.1080/17425247.2016.1218465.
23. Machado D, Girardini M, Viveiros M, Pieroni M. Challenging the Drug-Likeness Dogma for New Drug Discovery in Tuberculosis. Front Microbiol. 2018;9:1367. 10.3389/fmicb.2018.01367: 10.3389/fmicb.2018.01367.
24. Ma Z, Wang N, He H, Tang X. Pharmaceutical strategies of improving oral systemic bioavailability of curcumin for clinical application. J Control Release. 2019;316:359–80.10.1016/j.jconrel.2019.10.053: 10.1016/j.jconrel.2019.10.053.
25. Boutet E, Lieberherr D, Tognolli M, Schneider M, Bairoch A. UniProtKB/Swiss-Prot. Methods Mol Biol. 2007;406:89-112.10.1007/978-1-59745-535-0_4: 10.1007/978-1-59745-535-0$44.
26. Gfeller D, Grosdidier A, Wirth M, Daina A, Michielin O, Zoete V. SwissTargetPrediction: a web server for target prediction of bioactive small molecules. Nucleic Acids Res. 2014;42(Web Server issue):W32-8.10.1093/nar/gku293: 10.1093/nar/gku293.
27. Kim S, Chen J, Cheng T, Gindulyte A, He J, He S, et al. PubChem 2019 update: improved access to chemical data. Nucleic Acids Res. 2019;47(D1):D1102-d9.10.1093/nar/gky1033: 10.1093/nar/gky1033.
28. Ashburner M, Ball CA, Blake JA, Botstein D, Butler H, Cherry JM, et al. Gene ontology: tool for the unification of biology. The Gene Ontology Consortium. Nat Genet. 2000;25(1):25–9. 10.1038/75556: 10.1038/75556.

29. Ogata H, Goto S, Sato K, Fujibuchi W, Bono H, Kanehisa M. KEGG: Kyoto Encyclopedia of Genes and Genomes. Nucleic Acids Res. 1999;27(1):29–34.10.1093/nar/27.1.29: 10.1093/nar/27.1.29.
30. Bindea G, Mlecnik B, Hackl H, Charoentong P, Tosolini M, Kirilovsky A, et al. ClueGO: a Cytoscape plug-in to decipher functionally grouped gene ontology and pathway annotation networks. Bioinformatics. 2009;25(8):1091–3.10.1093/bioinformatics/btp101: 10.1093/bioinformatics/btp101.
31. Baek KH, Lee EJ, Kim YS. Recurrent pregnancy loss: the key potential mechanisms. Trends Mol Med. 2007;13(7):310–7.10.1016/j.molmed.2007.05.005: 10.1016/j.molmed.2007.05.005.
32. Lin MJ, Chen HW, Liu PH, Cheng WJ, Kuo SL, Kao MC. The prescription patterns of traditional Chinese medicine for women with polycystic ovary syndrome in Taiwan: A nationwide population-based study. Medicine. 2019;98(24):e15890.10.1097/md.0000000000015890: 10.1097/md.0000000000015890.
33. Smith SS. Female sex steroid hormones: from receptors to networks to performance–actions on the sensorimotor system. Prog Neurobiol. 1994;44(1):55. -86.10.1016/0301 – 0082(94)90057-4: 10.1016/0301 – 0082(94)90057-4.
34. Duan J, Yu Y, Li Y, Li Y, Liu H, Jing L, et al. Low-dose exposure of silica nanoparticles induces cardiac dysfunction via neutrophil-mediated inflammation and cardiac contraction in zebrafish embryos. Nanotoxicology. 2016;10(5):575–85.10.3109/17435390.2015.1102981: 10.3109/17435390.2015.1102981.
35. Wei J, Liu J, Liang S, Sun M, Duan J. Low-Dose Exposure of Silica Nanoparticles Induces Neurotoxicity via Neuroactive Ligand-Receptor Interaction Signaling Pathway in Zebrafish Embryos. Int J Nanomedicine. 2020;15:4407–15. 10.2147/ijn.S254480: 10.2147/ijn.S254480.
36. Graham CH, Hawley TS, Hawley RG, MacDougall JR, Kerbel RS, Khoo N, et al. Establishment and characterization of first trimester human trophoblast cells with extended lifespan. Experimental cell research. 1993;206(2):204–11.10.1006/excr.1993.1139: 10.1006/excr.1993.1139.
37. Li M, Wu X, An P, Dang H, Liu Y, Liu R. Effects of resveratrol on autophagy and the expression of inflammasomes in a placental trophoblast oxidative stress model. Life Sci. 2020;256:117890.10.1016/j.lfs.2020.117890: 10.1016/j.lfs.2020.117890.
38. Olson DM. The role of prostaglandins in the initiation of parturition. Best Pract Res Clin Obstet Gynaecol. 2003;17(5):717 – 30.10.1016/s1521-6934(03)00069 – 5: 10.1016/s1521-6934(03)00069 – 5.
39. Brodt-Eppley J, Myatt L. Prostaglandin receptors in lower segment myometrium during gestation and labor. Obstet Gynecol. 1999;93(1):89-93.10.1016/s0029-7844(98)00378-0: 10.1016/s0029-7844(98)00378-0.
40. Cook JL, Shallow MC, Zaragoza DB, Anderson KI, Olson DM. Mouse placental prostaglandins are associated with uterine activation and the timing of birth. Biol Reprod. 2003;68(2):579–87.10.1095/biolreprod.102.008789: 10.1095/biolreprod.102.008789.

41. Hirst JJ, Parkington HC, Young IR, Palliser HK, Peri KG, Olson DM. Delay of preterm birth in sheep by THG113.31, a prostaglandin F2alpha receptor antagonist. Am J Obstet Gynecol. 2005;193(1):256 – 66.10.1016/j.ajog.2004.11.009: 10.1016/j.ajog.2004.11.009.
42. Peri KG, Quiniou C, Hou X, Abran D, Varma DR, Lubell WD, et al. THG113: a novel selective FP antagonist that delays preterm labor. Semin Perinatol. 2002;26(6):389– 97.10.1053/sper.2002.37307: 10.1053/sper.2002.37307.
43. Matsumoto T, Sagawa N, Yoshida M, Mori T, Tanaka I, Mukoyama M, et al. The prostaglandin E2 and F2 alpha receptor genes are expressed in human myometrium and are down-regulated during pregnancy. Biochem Biophys Res Commun. 1997;238(3):838–41.10.1006/bbrc.1997.7397: 10.1006/bbrc.1997.7397.
44. Christiaens I, Zaragoza DB, Guilbert L, Robertson SA, Mitchell BF, Olson DM. Inflammatory processes in preterm and term parturition. J Reprod Immunol. 2008;79(1):50–7.10.1016/j.jri.2008.04.002: 10.1016/j.jri.2008.04.002.
45. Haas U, Sczakiel G, Laufer SD. MicroRNA-mediated regulation of gene expression is affected by disease-associated SNPs within the 3'-UTR via altered RNA structure. RNA Biol. 2012;9(6):924– 37.10.4161/rna.20497: 10.4161/rna.20497.
46. Tsygankova OM, Peng M, Maloney JA, Hopkins N, Williamson JR. Angiotensin II induces diverse signal transduction pathways via both Gq and Gi proteins in liver epithelial cells. J Cell Biochem. 1998;69(1):63–71.10.1002/(sici)1097–4644(19980401)69:1 < 63::aid-jcb7 > 3.0.co;2-t: 10.1002/(sici)1097–4644(19980401)69:1 < 63::aid-jcb7 > 3.0.co;2-t
47. Briet M, Barhoumi T, Mian MOR, Coelho SC, Ouerd S, Rautureau Y, et al. Aldosterone-Induced Vascular Remodeling and Endothelial Dysfunction Require Functional Angiotensin Type 1a Receptors. Hypertension. 2016;67(5):897-905.10.1161/hypertensionaha.115.07074: 10.1161/hypertensionaha.115.07074.
48. Zhao L, Dewan AT, Bracken MB. Association of maternal AGTR1 polymorphisms and preeclampsia: a systematic review and meta-analysis. J Matern Fetal Neonatal Med. 2012;25(12):2676– 80.10.3109/14767058.2012.708370: 10.3109/14767058.2012.708370.
49. Shah DM. The role of RAS in the pathogenesis of preeclampsia. Curr Hypertens Rep. 2006;8(2):144– 52.10.1007/s11906-006-0011-1: 10.1007/s11906-006-0011-1.
50. Vitoratos N, Hassiakos D, Iavazzo C. Molecular mechanisms of preeclampsia. J Pregnancy. 2012;2012:298343.10.1155/2012/298343: 10.1155/2012/298343.
51. Irani RA, Xia Y. The functional role of the renin-angiotensin system in pregnancy and preeclampsia. Placenta. 2008;29(9):763–71.10.1016/j.placenta.2008.06.011: 10.1016/j.placenta.2008.06.011.
52. Senbonmatsu T, Saito T, Landon EJ, Watanabe O, Price E Jr, Roberts RL, et al. A novel angiotensin II type 2 receptor signaling pathway: possible role in cardiac hypertrophy. Embo j. 2003;22(24):6471– 82.10.1093/emboj/cdg637: 10.1093/emboj/cdg637.
53. Renthal NE, Williams KC, Montalbano AP, Chen CC, Gao L, Mendelson CR. Molecular Regulation of Parturition: A Myometrial Perspective. Cold Spring Harb Perspect Med.

2015;5(11).10.1101/cshperspect.a023069: 10.1101/cshperspect.a023069.

54. Zeng Z, Velarde MC, Simmen FA, Simmen RC. Delayed parturition and altered myometrial progesterone receptor isoform A expression in mice null for Krüppel-like factor 9. Biol Reprod. 2008;78(6):1029–37.10.1095/biolreprod.107.065821: 10.1095/biolreprod.107.065821.
55. Mesiano S. Myometrial progesterone responsiveness and the control of human parturition. J Soc Gynecol Investig. 2004;11(4):193-202.10.1016/j.jsgi.2003.12.004: 10.1016/j.jsgi.2003.12.004.
56. Brown AG, Leite RS, Strauss JF. 3rd. Mechanisms underlying "functional" progesterone withdrawal at parturition. Ann N Y Acad Sci. 2004;1034:36–49. 10.1196/annals.1335.004: 10.1196/annals.1335.004.
57. Sykes L, MacIntyre DA, Teoh TG, Bennett PR. Anti-inflammatory prostaglandins for the prevention of preterm labour. Reproduction. 2014;148(2):R29–40. 10.1530/rep-13-0587: 10.1530/rep-13-0587.
58. Kuessel L, Grimm C, Knöfler M, Haslinger P, Leipold H, Heinze G, et al. Common oxytocin receptor gene polymorphisms and the risk for preterm birth. Dis Markers. 2013;34(1):51–6.10.3233/dma-2012-00936: 10.3233/dma-2012-00936.
59. Fuchs AR, Fuchs F, Husslein P, Soloff MS. Oxytocin receptors in the human uterus during pregnancy and parturition. Am J Obstet Gynecol. 1984;150(6):734–41.10.1016/0002-9378(84)90677-x: 10.1016/0002-9378(84)90677-x.
60. Xu YJ, Ren LD, Zhai SS, Ran LM, Hu LL, Luo XH, et al. OXTR and ZEB1 expression before and after progesterone dosing in pregnant women with threatened premature labor. Eur Rev Med Pharmacol Sci. 2017;21(14):3164–8.
61. Young IR. The comparative physiology of parturition in mammals. Front Horm Res. 2001;27:10–30.10.1159/000061036: 10.1159/000061036.
62. Hardy DB, Janowski BA, Corey DR, Mendelson CR. Progesterone receptor plays a major antiinflammatory role in human myometrial cells by antagonism of nuclear factor-kappaB activation of cyclooxygenase 2 expression. Mol Endocrinol. 2006;20(11):2724–33.10.1210/me.2006 – 0112: 10.1210/me.2006 – 0112.

Figures

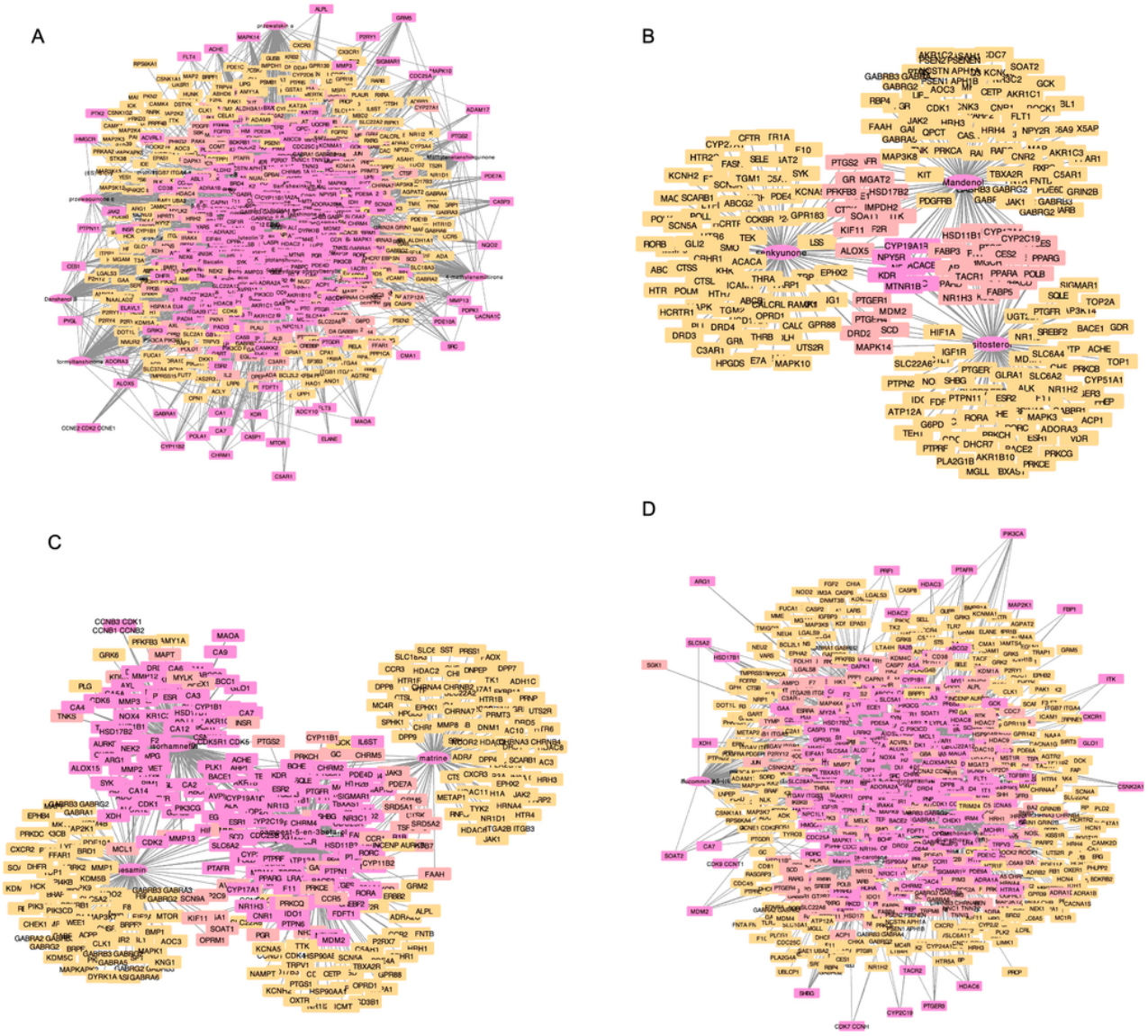

Figure 1

The ingredient-target networks of (A) Radix Salviae, (B) Chuanxiong Rhizoma, (C) Cuscutae Semen, and (D) Eucommiae Cortex. The circular nodes represent ingredients, and the square nodes represent targets. The colors of the nodes are illustrated from yellow to pink in ascending order of degree values.

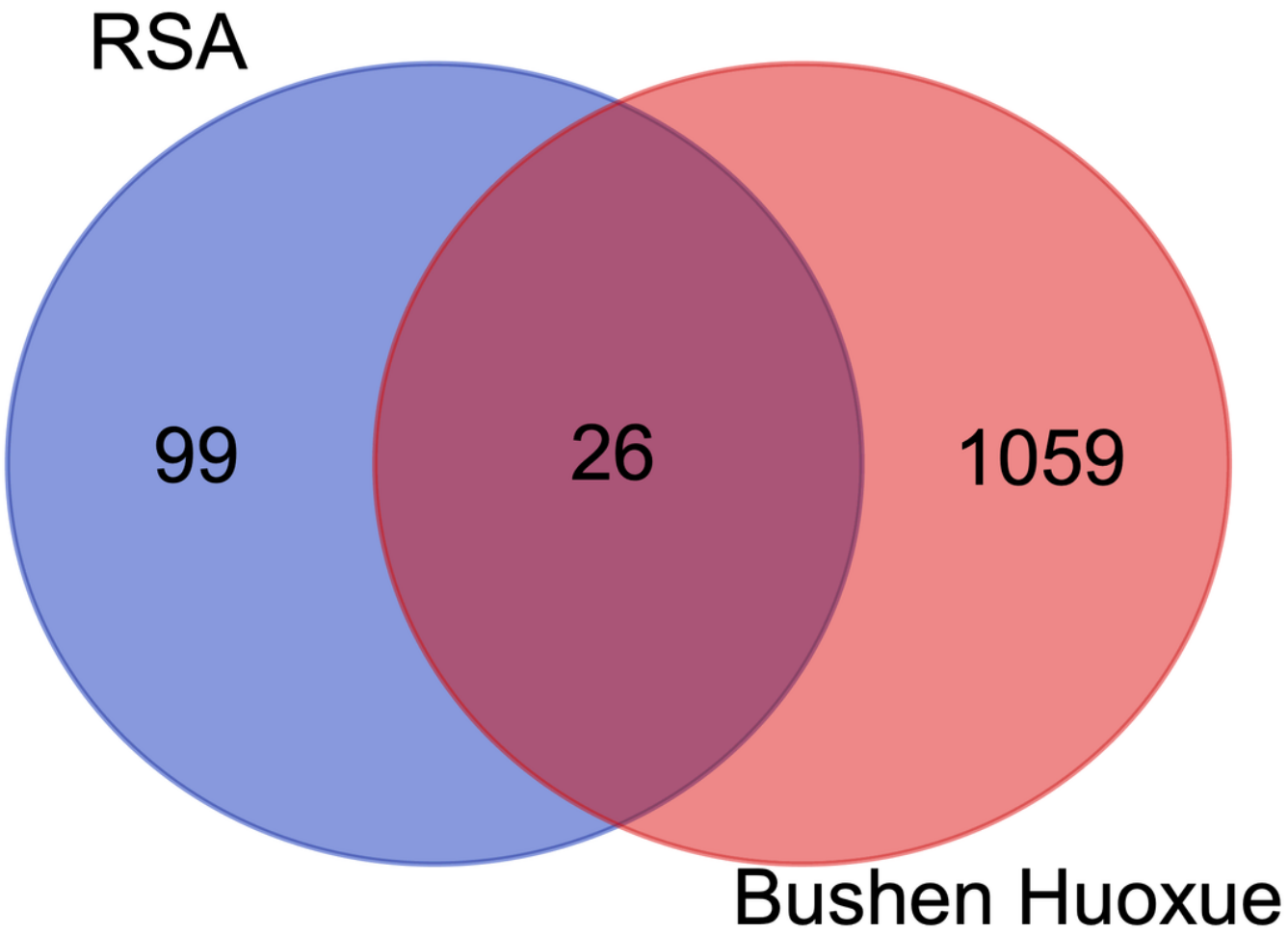

Figure 2

RSA-BHD common targets

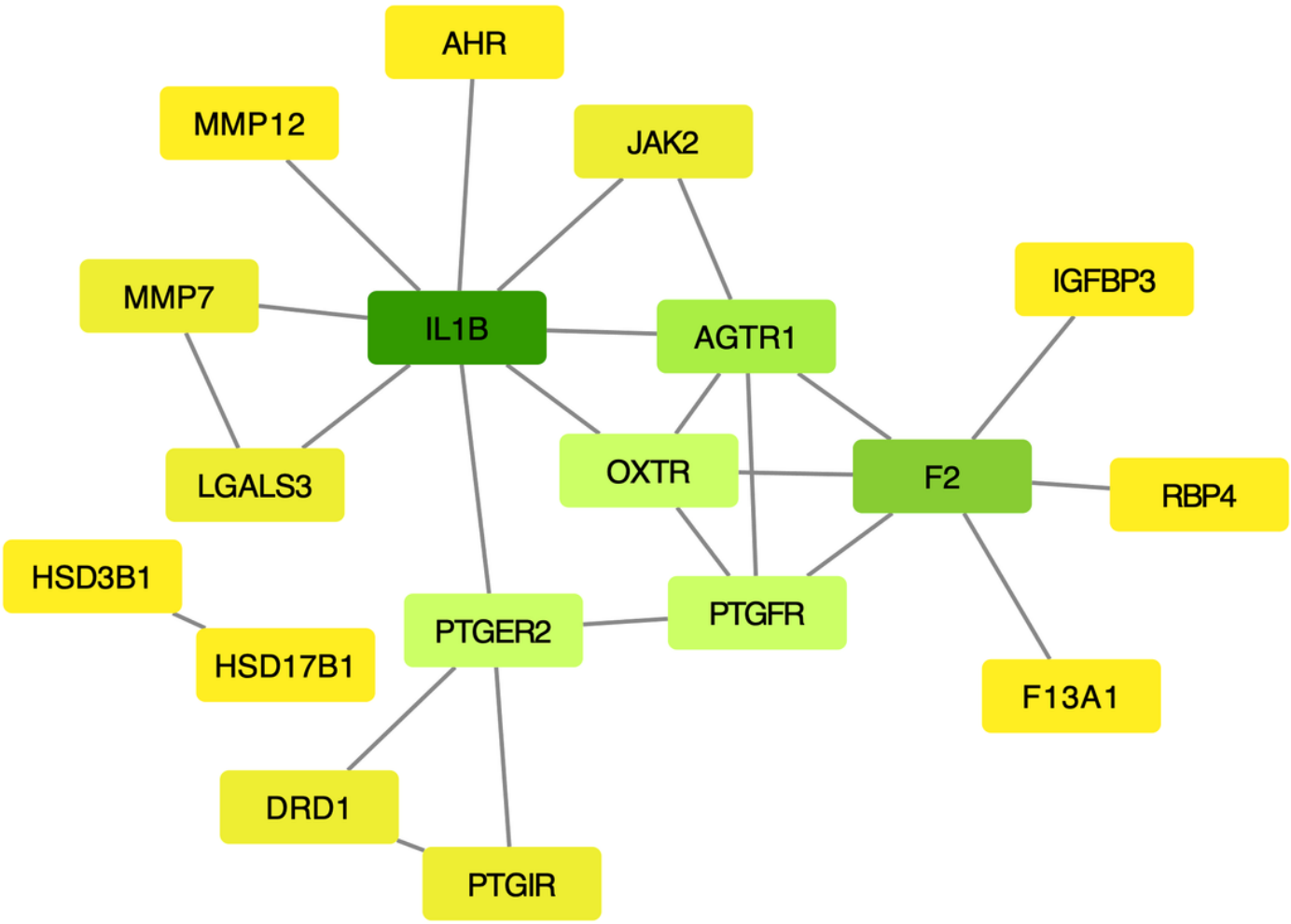

Figure 3

PPI network of targets for CDD in treating PCOS (from yellow to green, the degrees of freedom increase)

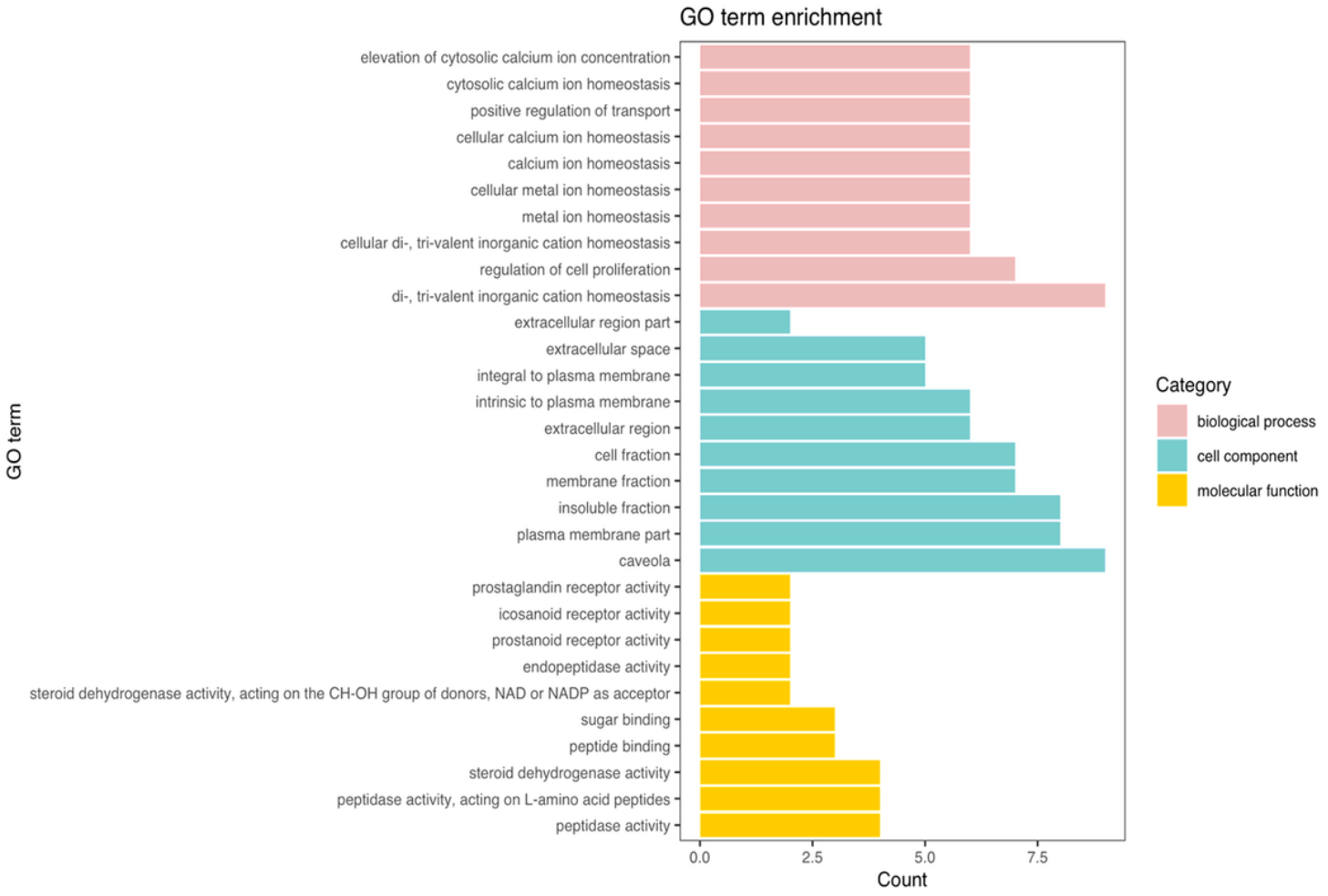

Figure 4

GO enrichment analysis of therapeutic targets of BHD in treating RSA

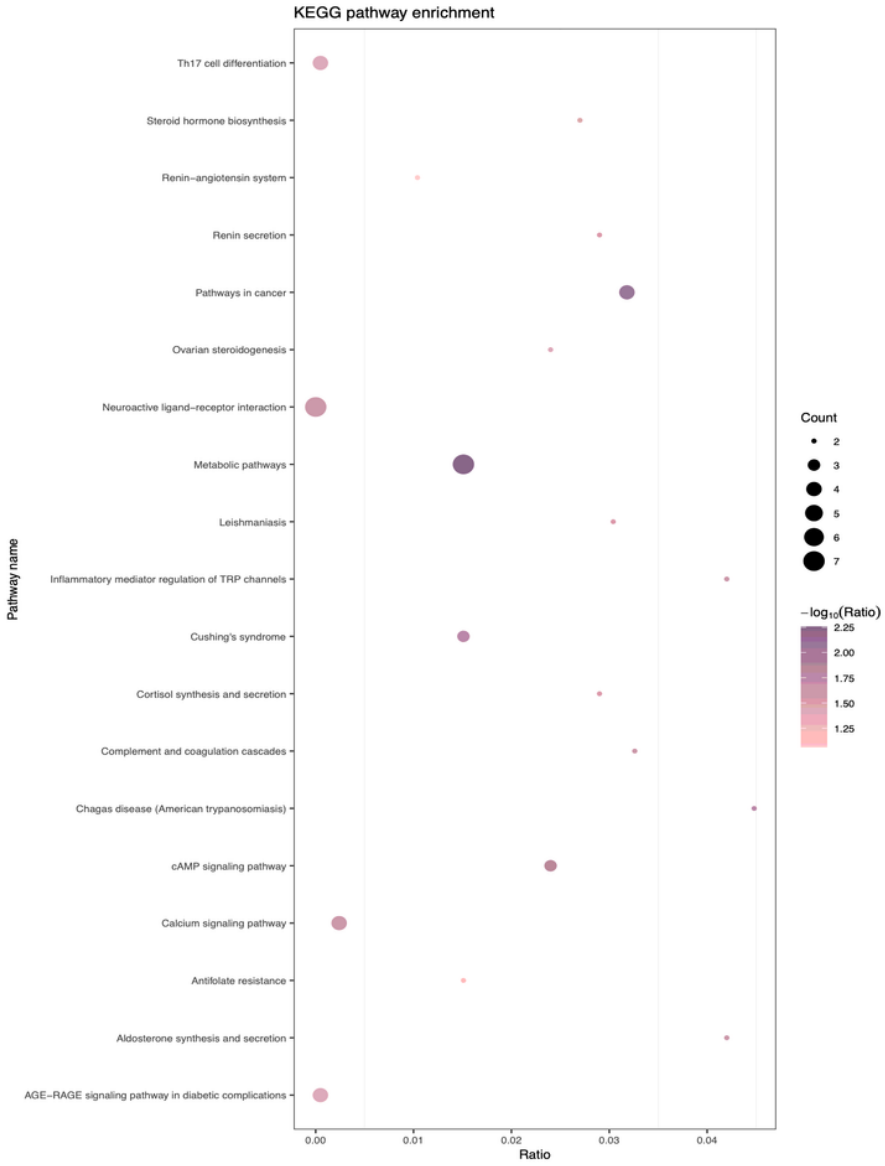

Figure 5

KEGG enrichment pathway analysis of therapeutic targets of BHD in treating RSA

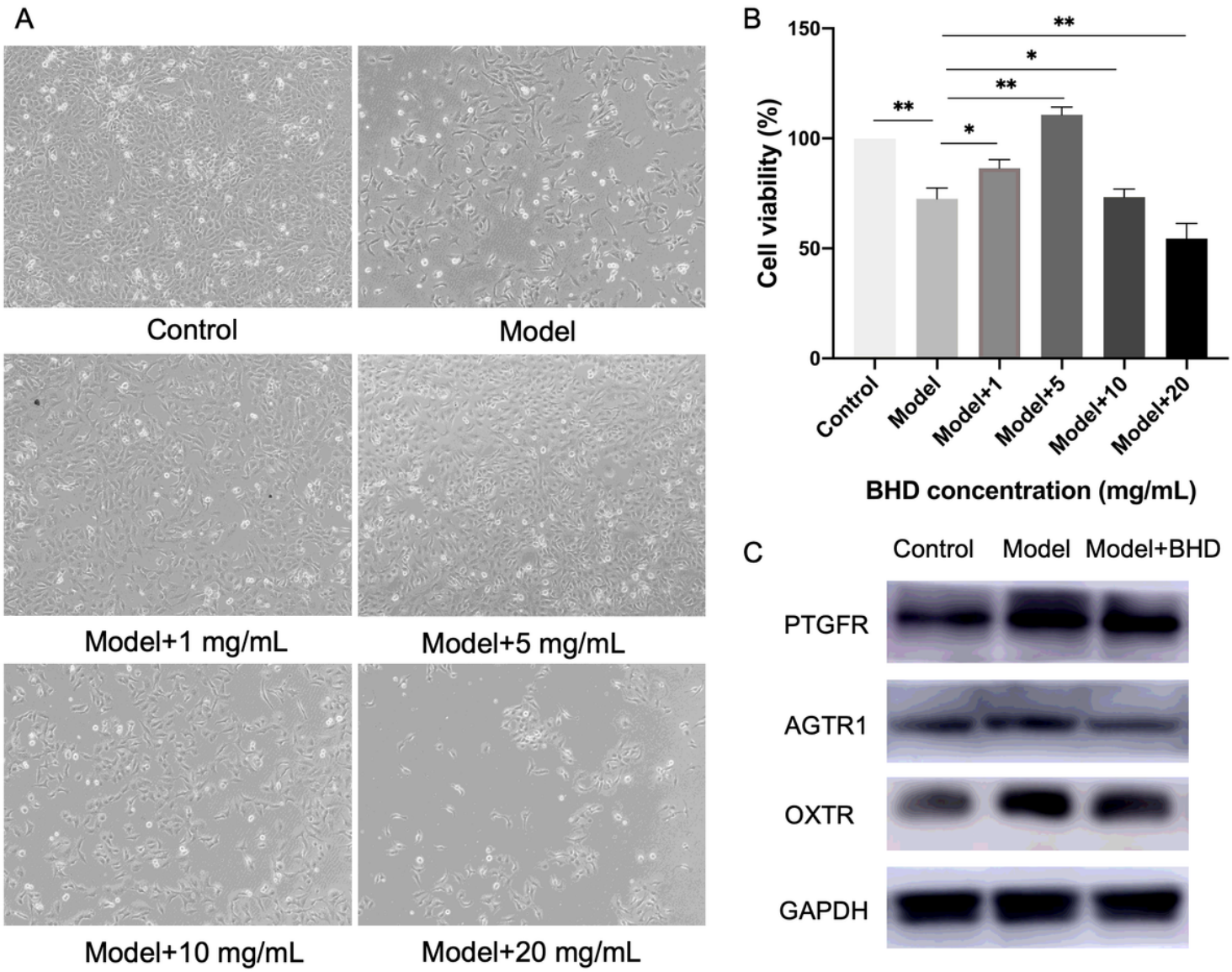

Figure 6

Determination of safe concentration of BHD water extract in HTR-8/SVneo cells A. Cell viability of HTR-8/SVneo cells pre-treated with 300 μmol/L H2O2 for 3 h followed by stimulation with varying doses of BHD (10, 50, 100, 200 mg/mL) for 48 h. (*P < 0.05, **P < 0.01). B. Representative images showing morphological changes by BHD in HTR-8/SVneo cells (200 ×magnification). C. Effects of BHD on PTGFR, AGTR1 and OXTR expression in HTR-8/SVneo cells RSA model detected by Western blot assay. Representative images are shown.

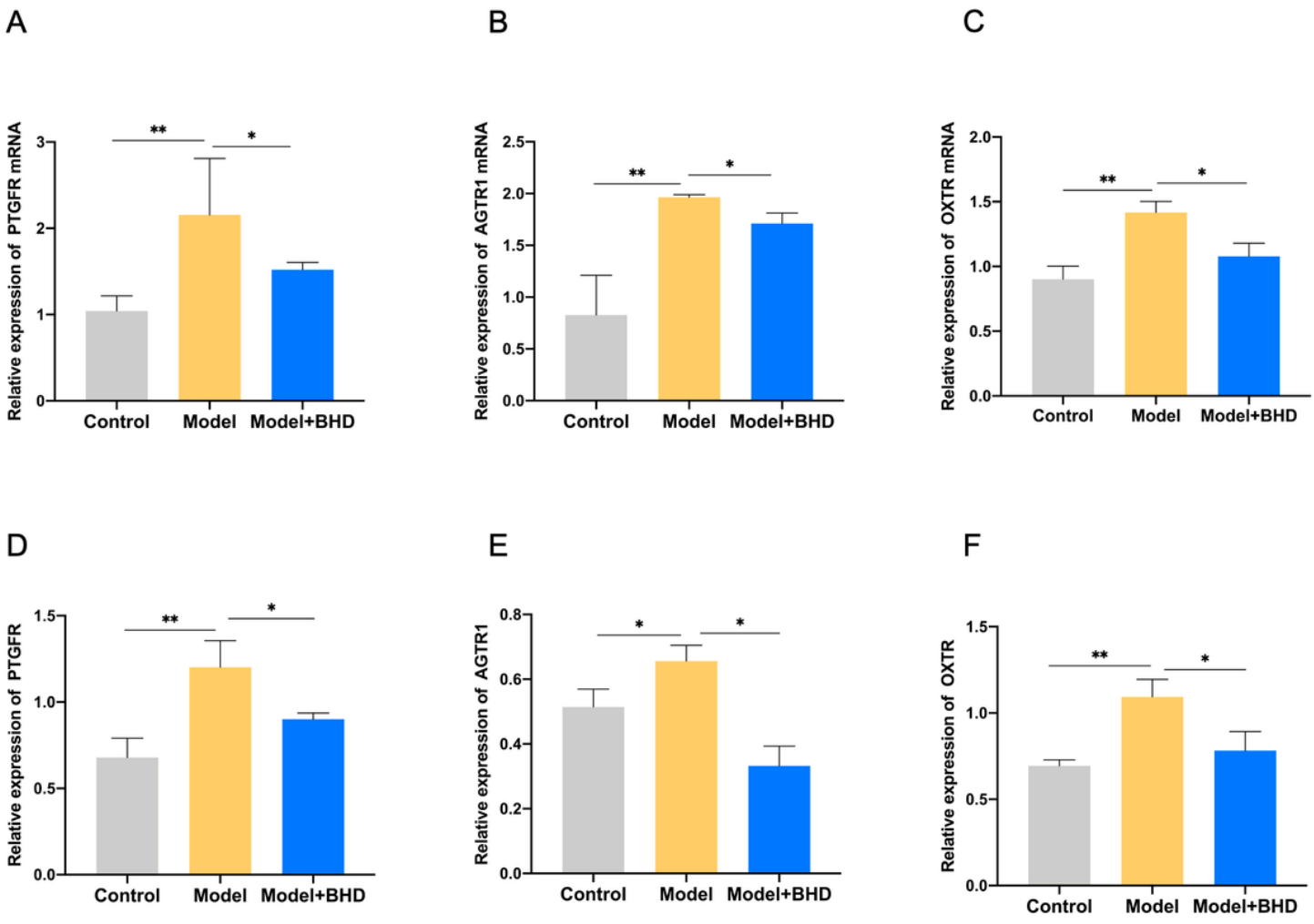

Figure 7

BHD participated in the treatment of RSA through the pathway A, B, C: qRT-PCR analyses of PTGFR, AGTR1 and OXTR mRNA in HTR-8/SVneo cells (*P < 0.05, **P < 0.01). D, E, F: The expression of protein PTGFR, AGTR1 and OXTR in HTR-8/SVneo cells were measured by Western blotting analysis. GAPDH was used as a normalization control. All group values are given as mean ± SD. (**P < 0.01, *P < 0.05).